LASER INTERFEROMETER GRAVITATIONAL WAVE OBSERVATORY
- LIGO -
CALIFORNIA INSTITUTE OF TECHNOLOGY
MASSACHUSETTS INSTITUTE OF TECHNOLOGY

Document Type	**LIGO-T970091-00 - D**	3/28/97

Determination of the Wedge Angles for the Core Optics Components

D. Coyne

Distribution of this draft:

Detector

This is an internal working note
of the LIGO Project.

California Institute of Technology
LIGO Project - MS 51-33
Pasadena CA 91125
Phone (818) 395-2129
Fax (818) 304-9834
E-mail: info@ligo.caltech.edu

Massachusetts Institute of Technology
LIGO Project - MS 20B-145
Cambridge, MA 01239
Phone (617) 253-4824
Fax (617) 253-7014
E-mail: info@ligo.mit.edu

WWW: http://www.ligo.caltech.edu/

Abstract

The wedge angles of the Core Optics Components (COC) have been determined. The criteria used to set the wedge angles, the method by which the angles have been calculated and the wedge angle values are documented in this report.

Keywords: core optics, wedge, optical layout, ghost beams, pickoff beams

1 OVERVIEW

The Core Optics Components (COC) consist of the Recycling Mirror (RM), Beamsplitter (BS), Folding Mirror (FM), Input Test Mass (ITM) and End Test Mass (ETM). These optics all have wedged surfaces to deflect ghost beams (due to internal reflections) off of the primary ray path so that they don't interfere with the main beam. In addition, the first reflections off of the anti-reflection (AR) coated surfaces of the ITM are used as pickoff beams for alignment sensing.

The basic criteria for setting the wedge angles, the methods by which they are calculated and the resulting values are given below. The proposed COC wedge angles were reviewed and approved in a meeting at Caltech[1] on March 20th.

2 CONSTRAINTS

The following constraints apply to the selection of the wedge angles:

1) The positions of the COC in planform (which sets the nominal distances between the COC) are defined by the choice of the Mode Cleaner (MC) cavity and the Recycling Cavity (RC) lengths and the Schnupp asymmetry; these positions have been defined in Ref. [1] and indicated in LIGO drawing D970003-00-D.

2) The nominal positions[2] of the 2km and 4km Interferometers (IFO) beams are 100 mm below the centerline of the BT and separated by 400 mm (200 mm left and right of the BT centerline), as indicated in LIGO drawing D970003-00-D.

3) The wedge angle for the Beamsplitter (BS) for the 2km and 4km interferometers are to be the same.

4) The wedge angle for the Recycling Mirror (RM) for the 2km and 4km interferometers are to be the same. This is made possible by using the angular alignment degrees of freedom of the Fold Mirrors (FM) in the 2 km IFO.

5) The maximum wedge angles for the optics are as follows:

---

1. Participants in the meeting were G. Billingsley, J. Camp, D. Coyne, W. Kells, S. Whitcomb, M. Smith. It was pointed out in the meeting that the wedge angles for the Recycling Mirrors (RM) should be the same for both the 2km and 4km interferometers (IFO); Subsequent to the meeting (and documented in this memorandum) a wedge angle solution was found, in which the Folding Mirrors (FM) of the 2km IFO are used to accommodate the RM wedge angle required for the 4km IFO. Otherwise all other COC wedge angles are as presented at the meeting.
2. These are only "nominal" positions of the beam within the BT aperture; the constraint to have identical wedge angles for ITMx and ITMy force the FP cavities to be slightly displaced vertically from these nominal positions. The precise positions are given later in this memo.

BS	1° 0′ maximum
ITM, RM	3° 0′ maximum

6) The wedge angle tolerance is ± 5′.

7) The BS, ITM and RM optics are symmetrically wedged, i.e. each surface is set at one-half the wedge angle relative to the cylindrical axis of the optic.

8) The ETM and FM optics are single surface wedged. The wedge angle for the ETM and FM are defined as 2° 0′ ± 5′. (The wedge angles for the ETM and FM are not critical since these optics are not used in transmission. The wedge was stipulated so that Pathfinder optics could be reused for the ETM and RM.)

9) The thickness of the core optics is defined as 100 mm at the thickest part of the wedge for the ITM (Ref.[2]) and RM (Ref.[3])and 40 mm at the thinnest part of the wedge for the BS (Ref. [4]).

10) The vertical positions of the HAM and BSC tables are as given in Figure 1. The dimensions in

Figure (1) Nominal Beam and Optics Table Elevation (taken from Ref. [5])

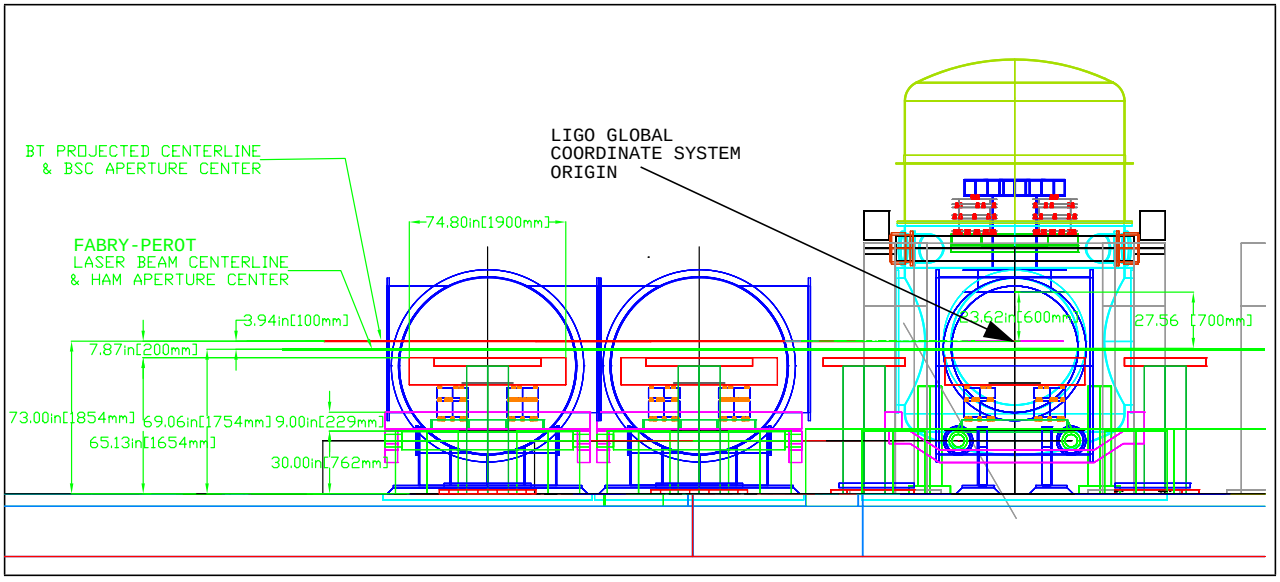

this figure are consistent with the heights of the optics tables defined in the SEI PDR (Ref.[6]).

11) The principal ray of the laser light entering the Recycling Mirror should be parallel to the plane defined by the BT axes (i.e. parallel to the LIGO global x-y plane).

3 CRITERIA

1) The first reflections off of the anti-reflection (AR) coated surfaces of the Input Test Masses (ITM) are used as pickoff beams for Alignment Sensing and Control (ASC) (Ref. [7]). These beams must be separated sufficiently to ensure that scattered light from the reflected beam does not contribute significantly to the interferometer noise. The COC diameter (25 cm) was selected at the 1ppm level (plus centering tolerance) in order to limit TEM_{00} mode diffraction loss to acceptable levels (Ref. [3]). Since the AR coating reflectance is ≤0.01, this criteria implies that the primary beam (at the 1 ppm radius) be separated from the pickoff beam (at the 100 ppm radius) by a

distance (≥50 mm) sufficient to accommodate a beam reducing telescope structure. (The Gaussian beam waist in the RC is taken as 36 mm, so that the corresponding 100ppm radius is 77 mm, the 1ppm radius is 95 mm and the sum is 172 mm.)

2) Similarly, the first ghost beams from each optic must be separated sufficiently from the next optic in proximity to its path to allow for structures to beam dump or baffle the beam.

3) The wedge angles must be chosen so that the height of the principal ray into the RM is above the HAM optics table by a minimum distance of 166 mm. The LOS1 structure (Ref.[9] positions the RM center at 166 mm above the HAM optics table. The SOS structure (Ref. [10]) positions the center of the optic at 130 mm above the table. The difference in height between the principal ray into the RM and the suspension structure supported heights will be accommodated with spacers.

4) The wedge angles must be chosen so that the height of the center of the BS is positioned no closer than 450 mm from the BSC optics table. The minimum distance from the center of the suspended optic to the attachment plane, associated with the LOS1 suspension, is 450 mm. The BS will be suspended from the LOS2 suspension structure which has yet to be designed, but will be similar to the LOS1 in vertical dimensions.

5) The orientation of the COC surfaces with respect to the local gravity vector causes a coupling of seismic and thermal vertical motion to length motion. The noise due to this coupling for the Recycling Cavity (RC) surfaces should be much smaller that the contribution due to the Fabry-Perot (FP) cavity surfaces. The allowable contribution to the noise floor for each RC surface was set at 1/10 of the contribution due to each FP surface (see Appendix 1).

4 COORDINATE SYSTEM

The orientation of the plane containing the interferometer arms, and the angle between the arms, is defined in the Refs. [11] and [12]. The LIGO global coordinate system (Ref. [11]) is defined with its coordinate axes aligned along the center of the BTs and its vertex at the projected intersection of these axes. The heights of the chambers and the SEI optics tables are adjusted so as to be locally level but at the proper position relative to the projected BT axes at their centers.

The optical ray tracing is done in a shifted coordinate system in which the center of the splitting surface of the 4km IFO BS is defined as the origin. Positions of the optical components are then transformed (shifted) to the LIGO global coordinate system, unless otherwise noted.

5 SOLUTION METHODS

Two methods[1] were used to independently confirm the wedge angles for the COC:

- vector analysis of the reflection and refraction (sequential ray tracing), and
- (non-sequential) optical ray tracing using Optica (Ref. [13]), including multiple internal reflections.

1. M. Smith also independently confirmed the ray angles and intercept positions using an independent spreadsheet analysis.

The wedge angles were calculated with the vector analysis as solutions to nonlinear, constraint equations and then confirmed with Optica. The vector analysis is described in Appendix 2.

6 SOLUTION

The wedge angles for the COC are given in Table 1. This set of wedge angles meets all of the constraints and criteria listed above.

Table 1: RC Core Optics Wedge Angles

(The End Test Mass (ETM) is listed for completeness, but is not part of this RC analysis.)

Optic	Wedge	
	Angle (deg)	Orientation of thick side
RM_{4k} RM_{2k}	2° 24′ (2.406)	down
BS_{4k} BS_{2k}	1° 0′ (1.000)	up
ITM_{4k}	1° 10′ (1.167)	up
ITM_{2k}	0° 34′ (0.567)	up
FM	2° 0′ (2.000)	up
ETM	2° 0′ (2.000)	up

A comparison to requirements (Table 2) indicates that the solution is acceptable.

Table 2: Layout Parameter Comparison with Requirements

Criteria #	Parameter	4km IFO (mm)	2km IFO (mm)	Requirement (mm)
1	ITM Pickoff Beam Separation from BS (margin after - R_{1ppm} - R_{100ppm})	108 ITMx 94 ITMy	106 ITMx 98 ITMy	≥ 50
2	ITM 1st ghost separation at the BS (margin after - R_{1ppm} - R_{100ppm})	115 ITMx 102 ITMy	110 ITMx 101 ITMy	≥ 50
	BS 1st ghost separation at the ITMs (margin after - R_{1ppm} - R_{100ppm})	27 ITMx[a] 37 ITMy	258 ITMx 206 ITMy	≥ ~50
	RM 1st ghost separation at the BS (margin after - R_{1ppm} - R_{100ppm})	362	203	≥ 50
3	Beam Height above the HAM table (SOS requires 140 mm min.)	226	186	≥ 166
4	Distance of the center of the beam-plitting surface of the BS below the BSC optics table mounting surface	657	615	≥ 450
5	RSS of length sensing noise due to wedge/orientation coupling from vertical seismic & thermal motion of RC surfaces (as a fraction of a FP surface contribution)	0.26	0.25	≤ 0.26
nominal constraint 2	Beam Vertical Distance Below the BT Centerline	101 ITMx 99 ITMy	101 ITMx 99 ITMy	~ 100

a. The beam separation margin between the BS 1st ghost and the primary beam at the ITMs for the 4km IFO is less than the desired 50mm, but is considered workable; the BS wedge angle is at the maximum manufacturing allowable of 1°.

The specific locations and orientations of the RC COC are given in Table 3.

Table 3: RC Core Optics Parameters

a) $\{\hat{i}, \hat{j}, \hat{k}\}$ are the coordinate system vector triad associated with the coordinate directions (x,y,z).
(b) The notation for points and unit normal vectors is per Figures 7 and 8 of Appendix 2.

Optic	Surface [a]	Center Coordinate				Surface Orientation (unit normal vector; direction cosines)			
		pt.	X (mm)	Y (mm)	Z (mm)	$\hat{n}$	$\hat{i}$	$\hat{j}$	$\hat{k}$
RM_{4k}	HR	p_3	-4596	212	26	$\hat{n}_3$	-0.999821	-0.000137	0.0188998
BS_{4k}	BS	p_4	-200	212	-57	$\hat{n}_4$	-0.70709	0.70709	0.00689
$ITM_{x,4k}$	HR	p_6	4677	200	-101	$\hat{n}_6$	-0.999793	0	-0.0203608
$ITM_{y,4k}$	HR	p_8	-200	4811	-99	$\hat{n}_8$	0	-0.999793	-0.0203608
RM_{2k}	HR	p_3	12184	9060	43	$\hat{n}_3$	0.999821	0	0.0188998
BS_{2k}	BS	p_4	9163	9060	-14	$\hat{n}_4$	0.70709	-0.70709	0.00689
FM_x	HR	p_9	9163	-200	-99	$\hat{n}_9$	0.706756	0.70745	0.0033158
$ITM_{x,2k}$	HR	p_{10}	9713	-200	-101	$\hat{n}_{10}$	-0.999951	0	-0.0098900
FM_y	HR	p_6	200	9072	-97	$\hat{n}_6$	0.707125	0.707081	0.0033196
$ITM_{y,2k}$	HR	p_7	200	9598	-99	$\hat{n}_7$	0	-0.999951	-0.0098900

a. HR = High Reflectance, BS = beamsplitting, AR = Anti-Reflectance

The unit length ray vectors (using the notation of Appendix 2) are given in Table 4.

Table 4: RC Core Optics Ray Parameters

Ray	Description	Ray unit vector (direction cosines)		
		$\hat{i}$	$\hat{j}$	$\hat{k}$
$\hat{u}_2$	RM input ray	1.0	0.000137	0
$\hat{u}_4$	BS input ray	0.999821	0.000137	-0.01889
$\hat{u}_6$	ITM_x input ray	0.999958	0	-0.009158
$\hat{u}_8$	ITM_y input ray	0	0.999958	-0.009158
$\hat{u}_2$	RM input ray	-1	0	0
$\hat{u}_4$	BS input ray	-0.999821	0	-0.0188998
$\hat{u}_9$	FM_x input ray	0.0001367	-0.999958	-0.0091561
$\hat{u}_{10}$	ITM_x input ray	0.99999	0	-0.004447
$\hat{u}_6$	FM_y input ray	-0.999958	0.0001367	-0.0091561
$\hat{u}_7$	ITM_y input ray	0	0.99999	-0.004447

The physical path length (not optical path length), folded into a common plane, versus elevation is given in Figures 2 and 3, for the 4km and 2km IFOs respectively.

Figure (2) 4km IFO Pathlength vs. Height

(a) The elevation origin is at the center of the splitting surface of the BS and not the LIGO global coordinate system origin.
(b) The path with reflection from the BS (red) is shorter than the path with transmission through the BS (green) due to the Schnupp asymmetry.

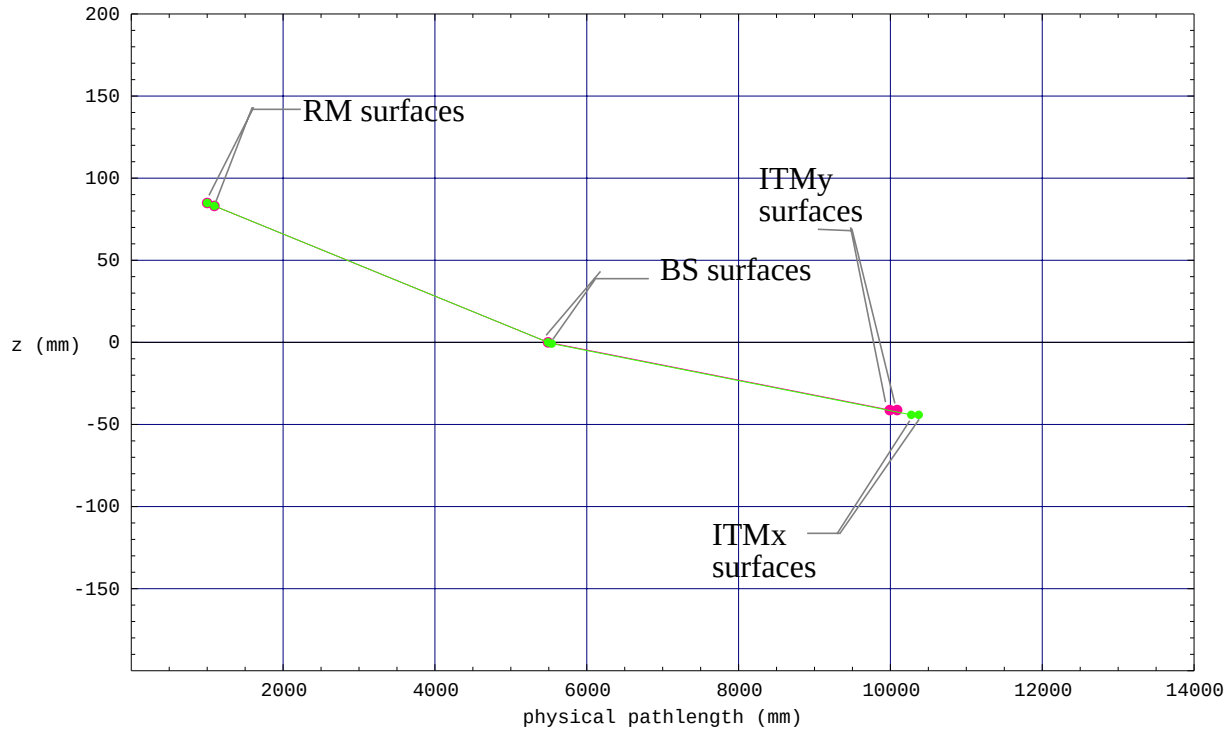

Figure (3) 2km IFO Pathlength vs. Height

(a) The elevation origin is at the center of the splitting surface of the BS and not the LIGO global coordinate system origin.
(b) The path with reflection from the BS (red) is longer than the path with transmission through the BS (green) due to the Schnupp asymmetry.

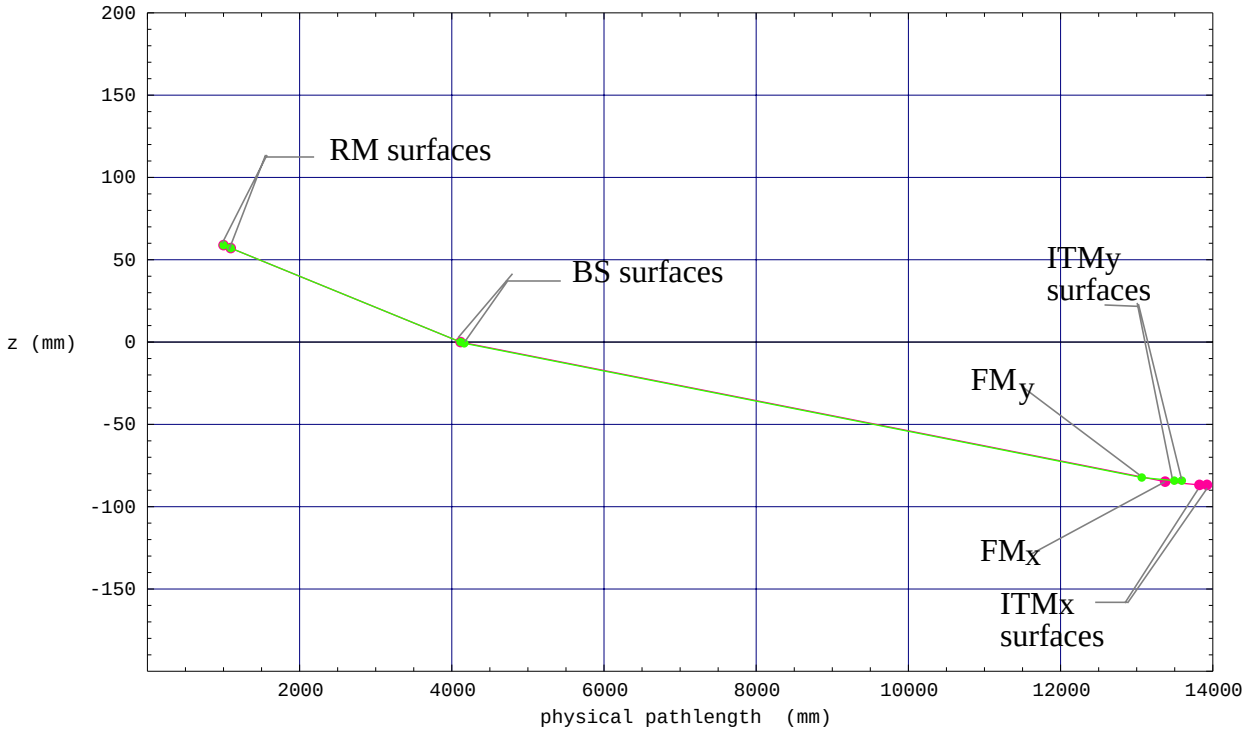

The 4km IFO RC optical layout in Optica is given in Figure 4.

Figure (4) Optica 4km IFO RC Layout (isometric view)

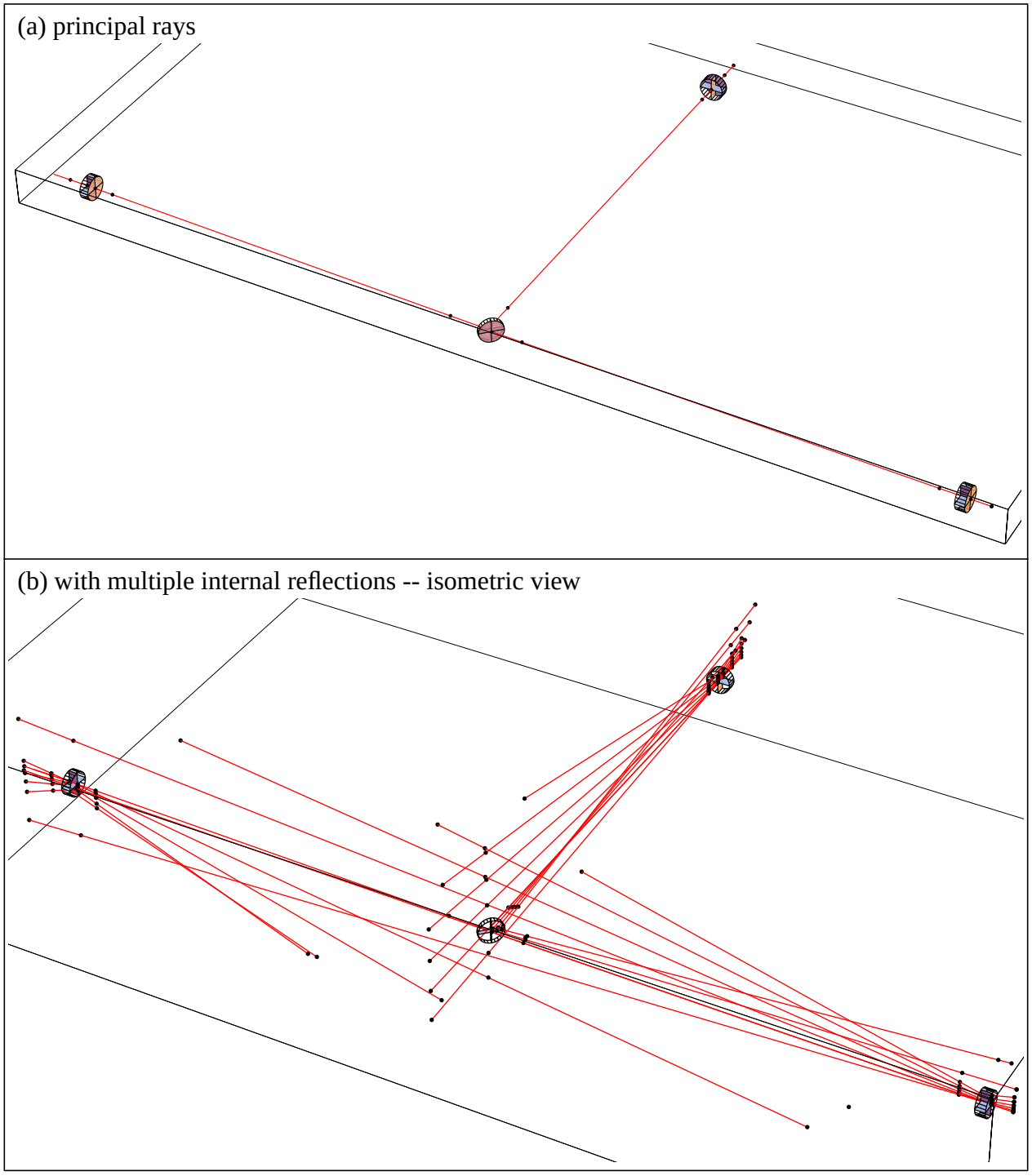

Figure (4) Optica 4km IFO RC Layout (isometric view)

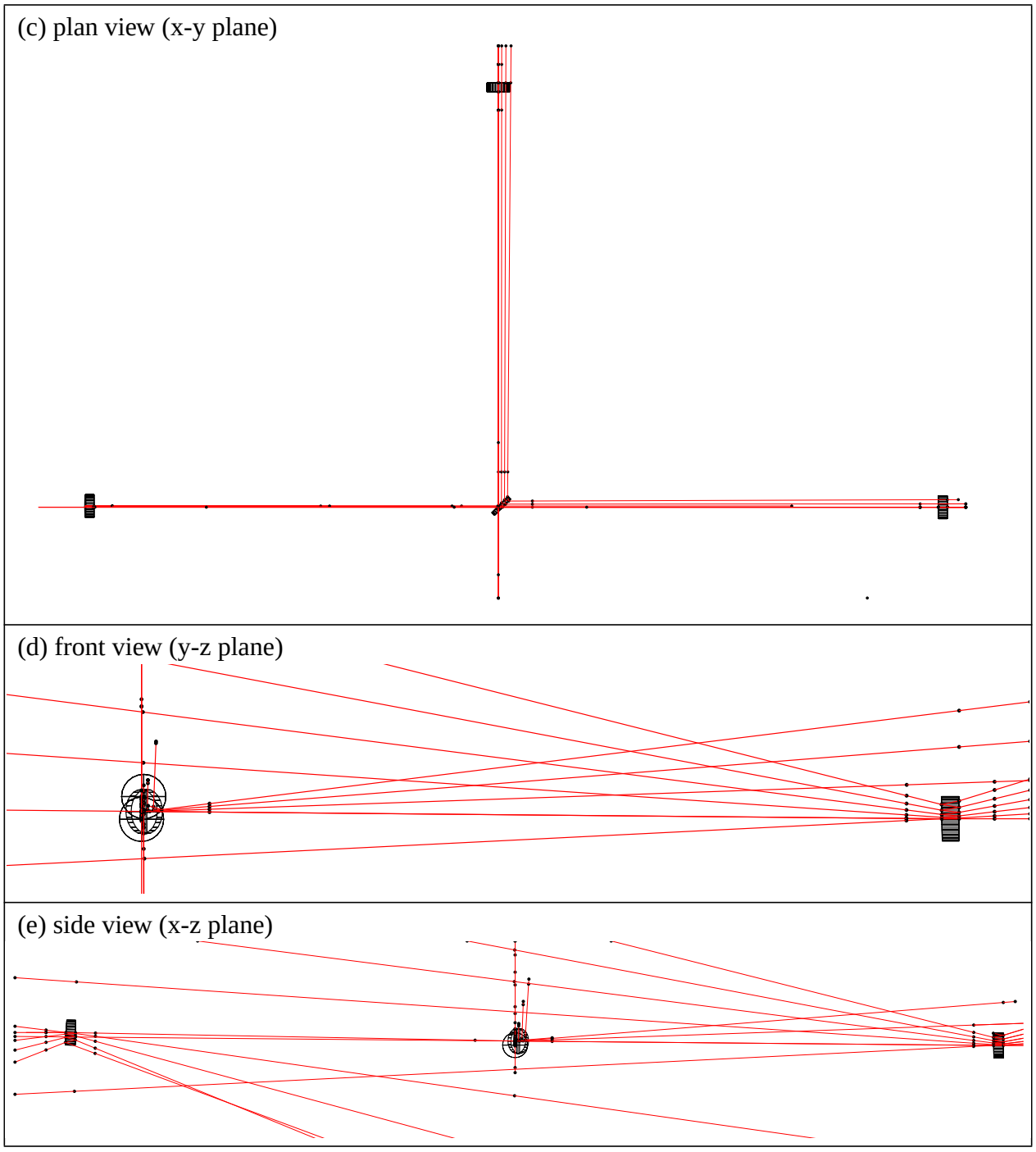

The 2km IFO RC optical layout in Optica is given in Figure 5.

Figure (5) Optica 2km IFO RC Layout (isometric view)

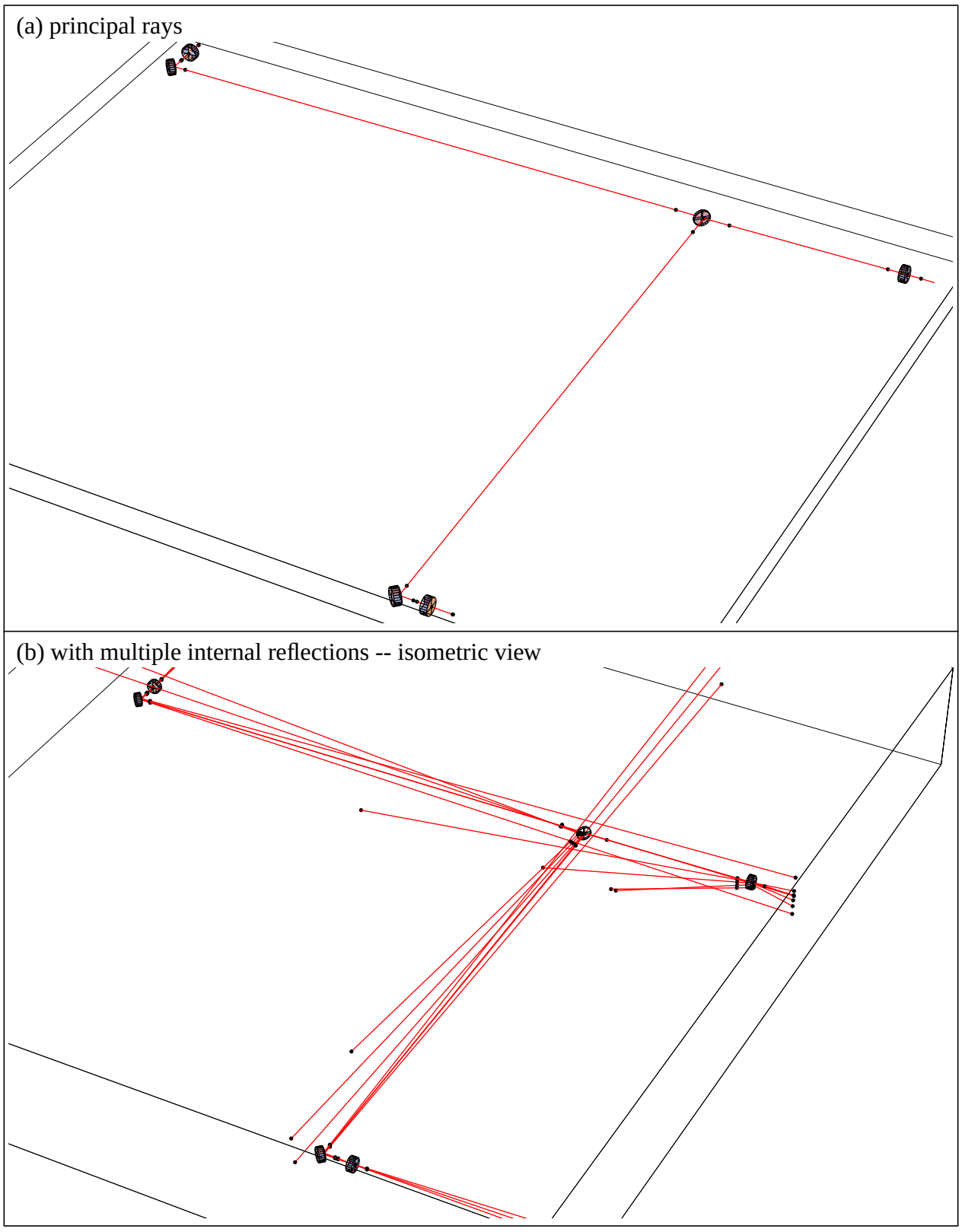

Figure (5) Optica 2km IFO RC Layout (isometric view)

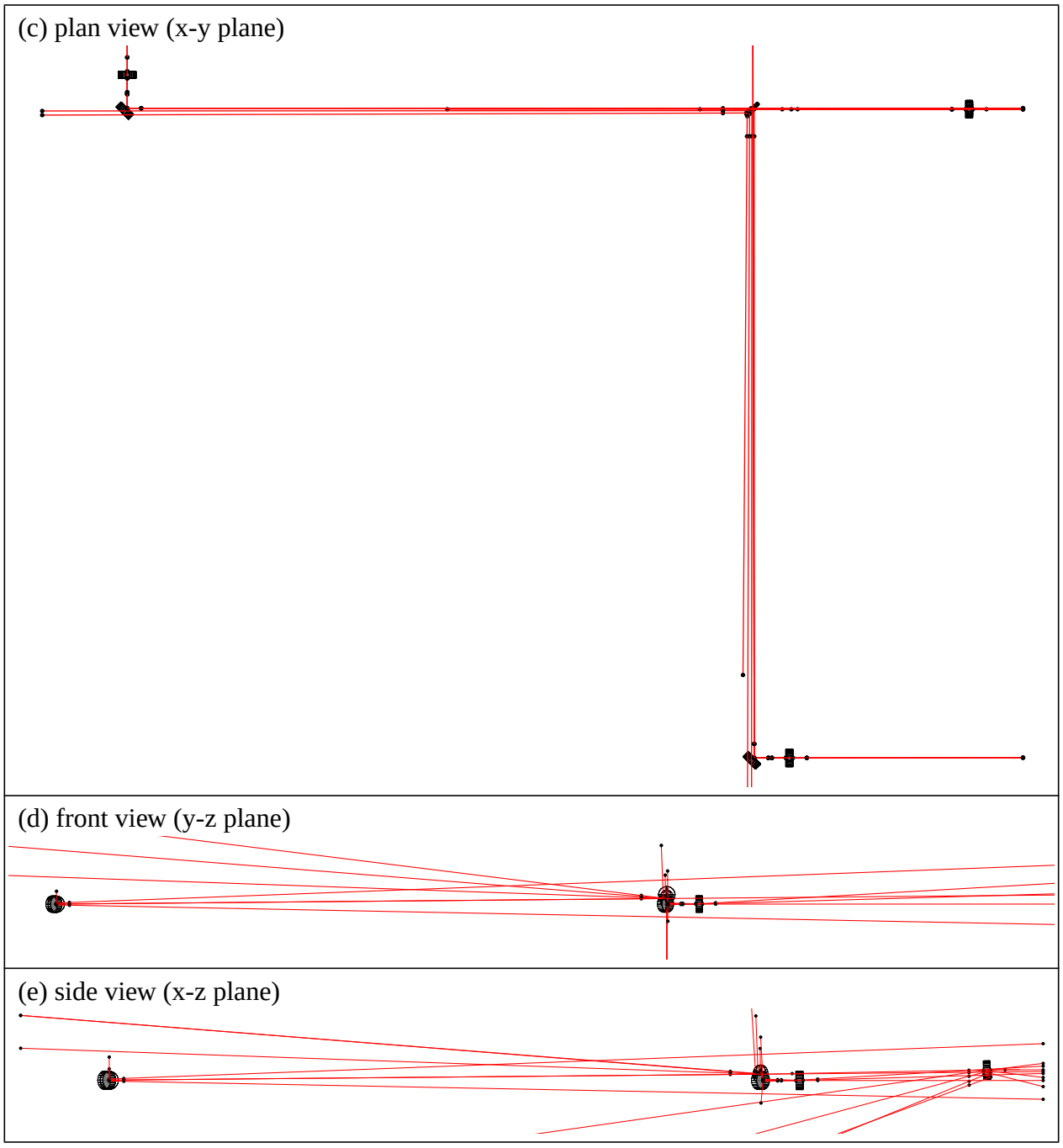

7 REFERENCES

[1] D. Coyne, “Recycling Cavity and Mode Cleaner Cavity Baseline Dimensions”, LIGO-T970068-00-D, 23 Feb 97.

[2] Input Test Mass Substrate, 4km IFO, LIGO-D960787-A-D.
Input Test Mass Substrate, 2km IFO, LIGO-D960803-A-D.

[3] Recycling Mirror Substrate, LIGO-D960785-A-D.

[4] Beamsplitter Substrate, LIGO-D960789-A-D.

[5] D. Shoemaker and D. Coyne, “Detector Subsystem Requirements Review”, LIGO-G960239-00-D, 4 Dec 96

[6] Seismic Isolation System (SEI) Preliminary Design Document, LIGO-C970257-00-D, Attachments:
(a) BSC Top Assembly SEI, drawing LIG-13000
(b) HAM Top Structure Assembly SEI, drawing LIG-20001 (with correction: from 65.24” to 65.13”)

[7] P. Fritschel, “Alignment Sensing/Control (ASC) Preliminary Design”, LIGO-T970060-00-D, 18 Feb 97.

[8] W. Kells, “Core Optics Components Requirements (1064 nm)”, LIGO-E950099-02-D, 1/29/96.

[9] PDR issue of the Large Optics Suspension, type 1 (LOS1) drawings, LIGO-D960132-00 (top level assembly drawing).

[10] PDR issue of the Small Optics Suspension (SOS) drawings, LIGO-D960001-00 (top level assembly drawing).

[11] A. Lazzarini, Determination of the as-built LIGO Global Coordinate Axes for Hanford, WA: Final analysis of the LIGO BT/VE interface survey monuments”, LIGO-T960176-C-E, 26 Nov 96.; This supersedes “Orientation of the Beam Tube Enclosure Foundation with Respect to the Local Horizontal: Hanford Site, LIGO-D950140-A, 28/11/95, which needs to be revised.

[12] “Orientation of the Beam Tube Enclosure Foundation with Respect to the Local Horizontal: Hanford Site, LIGO-D950140-A, 28 Nov 95

[13] D. Barnhart, “Optica: A New Generation System for Optical Design and Analysis”, version 1.1.0 with a patch for Mathematica 3.0, Wolfram Research, Jan 95.

APPENDIX 1 SEISMIC NOISE COUPLING

Vertical motion of the RC optics will couple into length noise if the surfaces are not vertical[1]. The seismic noise contribution due to coupling from vertical ITM motion to length change due to the earth's curvature (resulting in 0.6 mrad max. ITM HR surface angle relative to vertical) is significant. The wedge angles, which are required to separate ghost beams and provide angular alignment sensing beams (pickoff beams), cause the surfaces not to be vertical. The basic problem is to separate the ITM pickoff beam (and 1st ghost beam) at the BS by about 1 optic diameter:

$$\theta \approx \frac{\text{atan}\left(\frac{d}{l}\right)}{2} = \frac{\text{atan}\left(\frac{0.25}{4.5}\right)}{2} = 28 mrad \quad (1)$$

This ray deviation angle is large and suggests that there may be significant coupling from vertical motion to length signal (compare to 0.62 mrad in the Fabry-Perot cavities).

In transmission, vertical motion of a wedged optic causes a phase change due to an optical path difference (OPD). On the RC side, vertical motion of the ITM and the BS couple to the length sensing noise as follows:

$$\varphi_{(ITM,opd)} = \left(\frac{2\pi}{\lambda}\right)(n-1)\alpha_{ITM} z \quad (2)$$

$$\varphi_{(BS,opd)} = \left(\frac{2\pi}{\lambda}\right)(n-1)\alpha_{BS} z \quad (3)$$

where

n = index of refraction = 1.45
α_i = wedge angle of optic i
z = vertical motion (thermal or seismic)

Vertical motion of the reflective surfaces in the RC couple to the length sensing noise as follows:

$$\varphi_{BS} = \left(\frac{2\pi}{\lambda}\right)2\beta_{BS} z \quad (4)$$

$$\varphi_{FM} = \left(\frac{2\pi}{\lambda}\right)2\beta_{FM} z \quad (5)$$

1. Formulation due to D. Shoemaker and G. Gonzalez.

$$\varphi_{RM} = \left(\frac{2\pi}{\lambda}\right)\left(\frac{2\beta_{RM}}{CM}\right)z \tag{6}$$

where

β = angle from local vertical of the reflective surface of optic i
CM = common mode rejection factor = ~30

where the factor of 2 is due to mirror reflection. The motion of the recycling mirror itself is less bothersome for the GW output by the common mode rejection (CM) of the interferometer. The CM rejection is of the order of ~30 to ~100 (set CM = 30 to be conservative).

Motion of a HR ITM surface in the FP cavity contributes to the noise floor as follows:

$$\varphi_{fp} = \left(\frac{2\pi}{\lambda}\right)\beta_{fp}G_{fp}z \tag{7}$$

where

G_{fp} =130 = Fabry-Perot effective bounce factor, or phase change amplification

In general, the motion of the surfaces in the measurement band can be taken to be uncorrelated, so that the net contribution is the RSS of the individual contributions; the exceptions are the FMs. However, the FMs point in a different direction, so are at most $\sqrt{2}$ correlated, and they are probably not well correlated along their common axis. So as a simplification, we'll take all to be uncorrelated. The net noise contribution for the 2km IFO is then approximately:

$$\varphi_{total}^2 = \varphi_{RM}^2 + \varphi_{BS}^2 + 2\varphi_{FM}^2 + 4\varphi_{fp}^2 + 2\varphi_{(ITM,opd)}^2 + \varphi_{(BS,opd)}^2 \tag{8}$$

The same expression applies to the 4km IFO with the exception that there are no FMs in the 4km IFO. Rearranging this equation:

$$\xi = \left(\frac{\varphi_{total}^2}{\varphi_{fp}^2} - 4\right)^{1/2} = \left(\frac{\varphi_{RM}^2 + \varphi_{BS}^2 + 2\varphi_{FM}^2 + 2\varphi_{(ITM,opd)}^2 + \varphi_{(BS,opd)}^2}{\varphi_{fp}^2}\right)^{1/2} \le \frac{\sqrt{7}}{10} = 0.26 \tag{9}$$

Where we've taken as a criteria that each RC surface should contribute no more than 1/10 of the contribution of a FP surface.

The wedge and surface angles relative to vertical for the 2km and 4km IFOs are given in Table 5

Consequently,

$$\xi_{4k} = 0.26 \tag{10}$$

$$\xi_{2k} = 0.25 \tag{11}$$

Table 5. Optic Surface Angular Deviations (mrad) from Vertical

Optic (surface)		**2 km IFO**	**4km IFO**
RM(hr)	β	18.9	18.9
BS(bs)	β	6.9	6.9
	α	17.5	17.5
FMx(hr)	β	3.3	NA
ITMx(ar)	α	9.9	20.4
FMy(hr)	β	3.3	NA
ITMy(ar)	α	9.9	20.4

APPENDIX 2 VECTOR ANALYSIS

Consider a surface at which the index of refraction changes discretely (Fig. 6) and define a “natu-

Figure (6) Geometry for Refraction and Reflection at a Surface

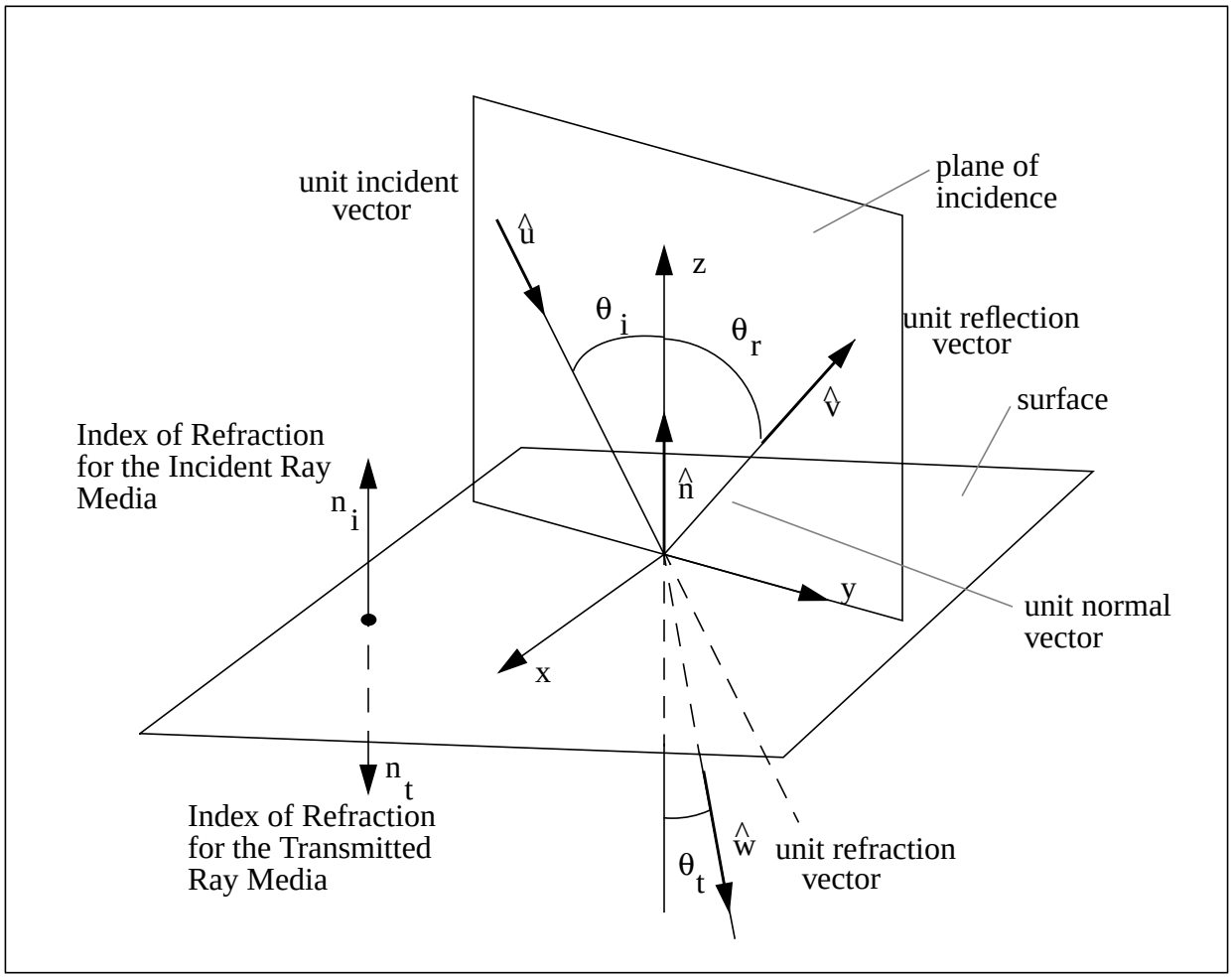

ral” coordinate system in the plane of incidence with the +z-axis coincident with the outward surface normal vector, $\hat{n}$, and the y axis at the intersection of the plane of incidence and the surface. Using the notation of Figure 6, and $\{\hat{i}, \hat{j}, \hat{k}\}$ as the coordinate system unit vector triad corresponding to {x,y,z}:

$$\hat{n} = \hat{k} \tag{12}$$

$$\hat{i} = \frac{\hat{u} \times \hat{n}}{|\hat{u} \times \hat{n}|} \tag{13}$$

$$\hat{j} = \hat{n} \times \hat{i} \tag{14}$$

The law of reflection is:

$$\Theta_i = \Theta_r \tag{15}$$

or,

$$\hat{v} = (\hat{u} \bullet \hat{j})\hat{j} - (\hat{u} \bullet \hat{k})\hat{k} \tag{16}$$

The law of refraction is:

$$n_i \sin\Theta_i = n_t \sin\Theta_t \tag{17}$$

or,

$$n_i(\hat{u} \bullet \hat{j}) = n_t(\hat{w} \bullet \hat{j}) \tag{18}$$

Since,

$$(\hat{w} \bullet \hat{k})^2 + (\hat{w} \bullet \hat{j})^2 = 1 \tag{19}$$

The refraction vector can be expressed as:

$$\hat{w} = \left(\frac{n_i}{n_t}\right)(\hat{u} \bullet \hat{j})\hat{j} - \left\{1 - \left(\frac{n_i}{n_t}\right)^2 (\hat{u} \bullet \hat{j})^2\right\}^{\frac{1}{2}} \hat{k} \tag{20}$$

These equations for reflection and refraction were defined as functions in Mathematica and used to propagate rays (unit vectors), $\hat{u}_m$, incident upon surface, S_m, into reflected rays, $\hat{v}_m$, and refracted rays, $\hat{w}_m$:

$$\hat{v}_m = Reflect[\hat{u}_m, \hat{n}_m] \tag{21}$$

$$\hat{w}_m = Refract[\hat{u}_m, \hat{n}_m, n_i, n_t] \tag{22}$$

The reflected rays and refracted rays then become the incident rays, $\hat{u}_{m+1}$, for the next surface, S_{m+1}.

The positions of the ray/surface intercept points are found by simply propagating the rays with the separation distances between the optics, $d_{(m+1)}$:

$$p_{(m+1)} = p_m + d_{m,(m+1)}\hat{u}_{(m+1)} \tag{23}$$

The surfaces of the optics in the 4km and 2 km IFOs are numbered as indicated in Figures 7 and 8,

Figure (7) Ray Vector Notation for the LIGO Recycling Cavity (4km IFO)

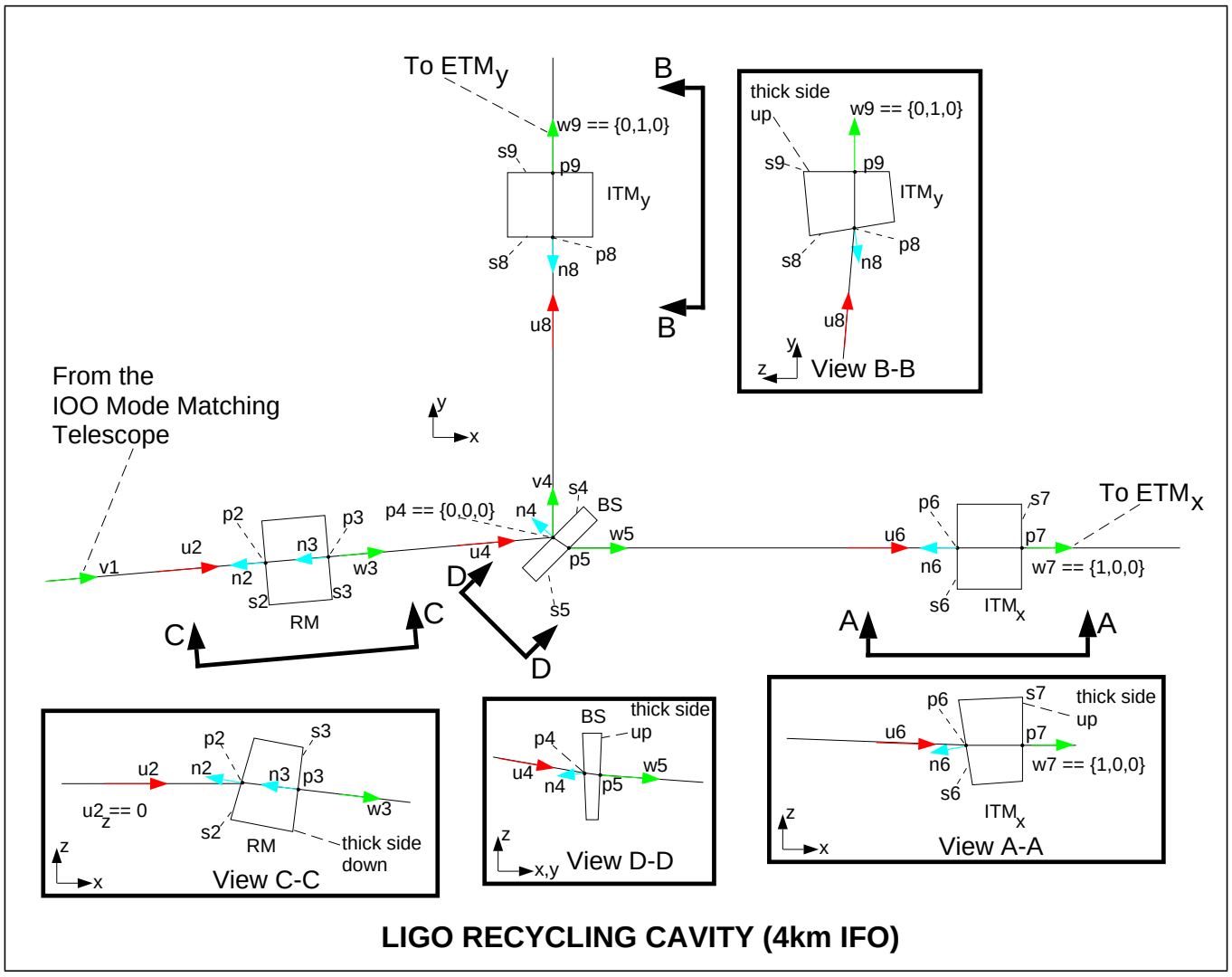

LIGO RECYCLING CAVITY (4km IFO)

respectively. The solution proceeds in stepwise fashion, first for the 4km IFO and then for the 2km IFO:

Step 1) The 4km IFO Fabry-Perot cavities are aligned along the coordinate axes, so that:

$$w_8 = u_9 = -v_9 = -n_9 = w_9 = \{0,1,0\} \tag{24}$$

$$w_6 = u_7 = -v_7 = -n_7 = w_7 = \{1,0,0\} \tag{25}$$

for the 4km IFO (and similarly for the 2km IFO).

Figure (8) Ray Vector Notation for the LIGO Recycling Cavity (2km IFO)

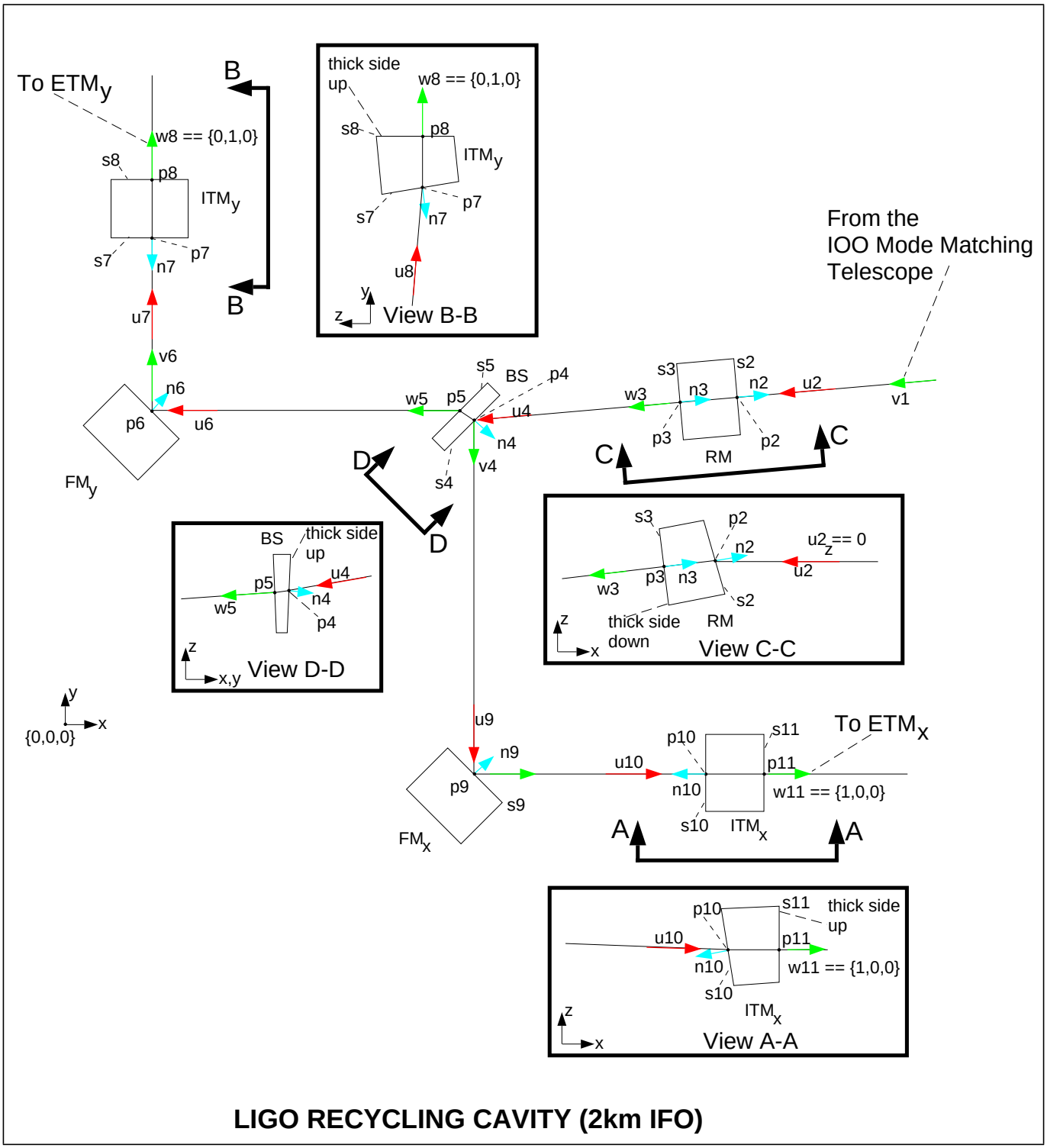

LIGO RECYCLING CAVITY (2km IFO)

Step 2) The wedge angles of the ITMx and ITMy optics were selected to give a first reflection off of the AR surface (i.e. vectors v_6 and v_8 for the 4km IFO and vectors v_7 and v_{10} for the 2km IFO) which meet criteria numbers 1 and 2. This turns out to be 1° 10′ for the 4km IFO and 0° 34′ for the 2 km IFO:

$$\hat{n}_8 = R_{\alpha_{8,9}} \hat{n}_9 \tag{26}$$

$$\hat{u}_8 = -Refract[-\hat{w}_8, -\hat{n}_8, n_{optic}, n_{vacuum}] \tag{27}$$

$$\hat{v}_8 = Reflect[\hat{u}_8, \hat{n}_8] \tag{28}$$

$$\delta_{8,4} = p_4 - (p_8 + d_{4,8}\hat{v}_8) \tag{29}$$

where

n_{optic} = 1.44963 @ λ = 1.064 mm for fused silica
n_{vacuum} = 1
R_θ = 3D rotation matrix for the angle θ
$\alpha_{m,m+1}$ = wedge angle for the optic with surfaces m and m+1

A similar equation applies for the rays associated with ITMx.

Step 3) With the BS output ray directions ($\hat{u}_8$ in reflection and $\hat{u}_6$ in transmission) determined, it is possible to calculate the BS orientation, $\hat{n}_4$, if a BS wedge angle, α_{45}, is assumed. Simultaneously solve:

$$\hat{u}_8 = Reflect[\hat{u}_4, \hat{n}_4] \tag{30}$$

$$\hat{u}_6 = Refract[Refract[\hat{u}_4, \hat{n}_4, n_{vacuum}, n_{optic}], \hat{n}_5, n_{optic}, n_{vacuum}] \tag{31}$$

given,

$$\hat{n}_5 = R_{\alpha_{4,5}} \hat{n}_4 \tag{32}$$

This is effectively 2 equations in 2 unknowns (the ‘tip’ and ‘tilt’ of the BS, $\hat{n}_4$). The assumed BS wedge angle, α_{45}, is checked (iterated) to assure that the first ghost beams are well separated from the ITMs (criteria 2). The result of this step is not only the BS orientation normal vector, $\hat{n}_4$, but also the input ray normal vector, $\hat{u}_4$.

Step 4) With the input ray vector to the BS known, $\hat{u}_4$, the stipulation that the RM HR surface be oriented in this direction (since it forms an input mirror for the RC) and the requirement that the input to the RM (i.e. the output of the IO mode matching telescope) be oriented parallel to the x-y global plane, we can determine the RM wedge angle:

$$\hat{w}_2 = \hat{u}_3 = \hat{w}_3 = \hat{u}_4 \tag{33}$$

$$\hat{n}_3 = -\hat{w}_2 \tag{34}$$

$$\hat{n}_2 = R_{\alpha_{2,3}} \hat{n}_3 \tag{35}$$

$$\hat{u}_2 = -Refract[-\hat{w}_2, -\hat{n}_2, n_{optic}, n_{vacuum}] \tag{36}$$

The RM wedge angle, α_{23}, is determined by minimizing the z component of the input ray vector to the RM:

$$\hat{u}_2 \bullet \hat{k} \equiv 0 \tag{37}$$

Step 5) Having determined the RM wedge angle for the 4km IFO, it is used in the 2km IFO. The ray vector through the RM and into the BS as well as the ray vectors into each of the ITMs are known. In addition, the orientation of the BS for the 2km IFO is defined to be the same as for the 4km IFO (i.e. setting the normal vector $\hat{n}_4$ to be the same for both IFOs). The FM orientation is then determined by simultaneous solution of the following equations:

$$\hat{u}_{10} \bullet \hat{j} \equiv \hat{v}_9 \bullet \hat{j} = Reflect[Reflect[\hat{u}_4, \hat{n}_4], \hat{n}_9] \bullet \hat{j} \tag{38}$$

$$\hat{u}_{10} \bullet \hat{k} \equiv \hat{v}_9 \bullet \hat{k} = Reflect[Reflect[\hat{u}_4, \hat{n}_4], \hat{n}_9] \bullet \hat{k} \tag{39}$$

$$\hat{u}_7 \bullet \hat{i} \equiv \hat{v}_6 \bullet \hat{i} = Reflect[Refract[Refract[\hat{u}_4, \hat{n}_4, n_{vacuum}, n_{optic}], \hat{n}_5, n_{optic}, n_{vacuum}], \hat{n}_6] \bullet \hat{i} \tag{40}$$

$$\hat{u}_7 \bullet \hat{k} \equiv \hat{v}_6 \bullet \hat{k} = Reflect[Refract[Refract[\hat{u}_4, \hat{n}_4, n_{vacuum}, n_{optic}], \hat{n}_5, n_{optic}, n_{vacuum}], \hat{n}_6] \bullet \hat{k} \tag{41}$$

These 4 equations are used to define the orientation of FM_x, $\hat{n}_9$, and FM_y, $\hat{n}_6$.